Frequency Calibration of A/D Converter in Software GPS Receivers

L. L. Liou, D. M. Lin, J. B. Tsui J. Schamus
Sensor Directorate
Air Force Research Laboratory

J. T. Morton
Department of Electrical Engineering
Miami University, Oxford, OH

Abstract--- **This paper presents a software-based method to calibrate Analog-to-digital converter (ADC) sampling frequency in a software GPS receiver. Two front-end systems of a GPS software receiver were used in this study. The sampling frequencies of the ADC were found deviated from the nominal values provided by the manufacturers. Software algorithm was developed to calibrate the sampling frequencies. The algorithm is based on the initial-code-phase velocity and the carrier-phase velocity of the GPS signals at L1 frequency obtained by software receiver measurements. Allan variance analysis of this frequency characterization method is also included in this study.**

I. INTRODUCTION

A typical radio frequency front-end of a software Global Positioning System (GPS) receiver includes an antenna, amplifiers, local oscillator(s), mixers, and an analog-to-digital converter (ADC). The GPS signals were received, amplified, down-converted, and digitized into base band samples. The base band samples are then processed using software routines to generate the receiver position information. These software routines typically achieve three operational functions: GPS signal acquisition, tracking, and position calculation. The accuracy and stability of the frequency source(s) in the front-end hardware affect both the IF and ADC sampling frequencies. The uncertainty in the sampling frequency will further propagate into the uncertainty in the carrier and Doppler frequencies. The larger the frequency uncertainty, the more frequency bins need to be searched in order to find the right Doppler. As a consequence, it takes longer time to perform data acquisition. During the tracking operation, the frequency source instability may lead to unstable ticking position between navigation bits which will cause errors in ephemeris parameters. As a result, the receiver position solutions may be either erroneous or completely unachievable.

In most commercial GPS receivers, the sampling frequency of an ADC provided by the manufacturer is of a nominal value. The true sampling frequency is usually resolved or characterized by using a standard frequency counter. In this study, we developed a software algorithm for the frequency characterization without using any additional hardware except those components described in the front-end of the GPS receiver. This algorithm is based on the properties of the GPS satellite C/A code and of the specific frequency plan in the system's circuit design. The frequency characterization process is integrated into the software receiver.

The frequency calibration techniques described in this report is essentially a technique of time and frequency transfer using GPS signals. This technique is made possible because that GPS precision time keeping capability is continuously maintained and the signals are available globally at most of the time. While most GPS time and frequency transfer uses hardware approach, this study uses a unique software approach. The advantage of the software approach is its flexibility to implement advanced algorithms for the purpose of enhancing signal-to-noise ratio or of adopting new signals when they become available.

II. EXPERIMENT

Two GPS receiver front-ends were used in this study. One is a custom-designed and developed system and the other is a commercial-modified system. The former contains two high quality frequency sources as shown in Fig. 1. One source is used as a local oscillator, and the other is used to control sampling frequency of an ADC. The first frequency source down-converts the GPS's L_1 frequency (f_L = 1.57542 GHz) to 21.25 MHz. The second frequency source feeds a sampling frequency of 5 MHz into ADC. The schematic frequency plan for this custom system is shown in Fig. 1.

The commercial-modified system contains one frequency source, two mixers, one ADC, and a sequence of multiply and division circuits as shown in Fig. 2. The primary frequency source is operating at a nominal frequency of 16.368 MHz. Through multiply circuits, it feeds 1.6368 GHz into the first mixer and 65.472 MHz into the second mixer. Through a division circuit, it feeds 5.456 MHz into the ADC as a sampling frequency. The nominal IF and base-band frequencies are also shown in Fig. 2.

0-7803-9052-0/05/$20.00 © 2005 IEEE.

Report Documentation Page

Form Approved
OMB No. 0704-0188

1. REPORT DATE	2. REPORT TYPE	3. DATES COVERED
AUG 2005		**00-00-2005 to 00-00-2005**

4. TITLE AND SUBTITLE	5a. CONTRACT NUMBER
Frequency Calibration of A/D Converter in Software GPS Receivers	5b. GRANT NUMBER
	5c. PROGRAM ELEMENT NUMBER
6. AUTHOR(S)	5d. PROJECT NUMBER
	5e. TASK NUMBER
	5f. WORK UNIT NUMBER
7. PERFORMING ORGANIZATION NAME(S) AND ADDRESS(ES) **Air Force Research Laboratory,Sensor Directorate,Wright Patterson AFB,OH,45433**	8. PERFORMING ORGANIZATION REPORT NUMBER
9. SPONSORING/MONITORING AGENCY NAME(S) AND ADDRESS(ES)	10. SPONSOR/MONITOR'S ACRONYM(S)
	11. SPONSOR/MONITOR'S REPORT NUMBER(S)

12. DISTRIBUTION/AVAILABILITY STATEMENT
Approved for public release; distribution unlimited

13. SUPPLEMENTARY NOTES
Joint IEEE International Frequency Symposium and Precise Time and Time Interval (PTTI) Systems and Applications Meeting, 29-31 Aug 2005, Vancouver, BC, Canada

14. ABSTRACT
This paper presents a software-based method to calibrate Analog-to-digital converter (ADC) sampling frequency in a software GPS receiver. Two front-end systems of a GPS software receiver were used in this study. The sampling frequencies of the ADC were found deviated from the nominal values provided by the manufacturers. Software algorithm was developed to calibrate the sampling frequencies. The algorithm is based on the initial-code-phase velocity and the carrier-phase velocity of the GPS signals at L1 frequency obtained by software receiver measurements. Allan variance analysis of this frequency characterization method is also included in this study.

15. SUBJECT TERMS

16. SECURITY CLASSIFICATION OF:			17. LIMITATION OF ABSTRACT	18. NUMBER OF PAGES	19a. NAME OF RESPONSIBLE PERSON
a. REPORT **unclassified**	b. ABSTRACT **unclassified**	c. THIS PAGE **unclassified**	**Same as Report (SAR)**	**8**	

III. FREQUENCY CALIBRATION ALGORITHM

1. C/A code Correlation

The civilian GPS signals were used in this study. The civil GPS signals have a carrier frequency at L1 band and are modulated by pseudorandom codes from the Gold code family, the C/A codes. The C/A code is a bi-phase code with a chipping rate of 1.023 MHz. The period of the code is 1 millisecond. The GPS software receiver's front-end generates digitized data. The digital data can then be processed using software algorithms on a block basis. Each block contains a millisecond of digital samples. A software acquisition routine was developed to correlate the measured digital data with a locally generated reference signal consisting of a base-band CW signal modulated by a C/A code sequence [1]. The reference signal's base-band frequency was allowed to vary within a reasonable range so that to cover a possible Doppler value. Fig. 3 shows a typical correlation result. For each millisecond of data, the initial C/A code phase represented by the initial code index (e.g., the sequential order of the data points, and it is not necessarily an integer) and a coarse Doppler frequency can be obtained from the correlation results. These parameters can be used to demodulate the input signal and to obtain an average carrier phase for the one millisecond data block. This block-based process is carried out for several seconds of data to yield distributions of the initial C/A code phase vs. time and the carrier phase vs. time.

2. The initial code phase velocity

A typical result of the initial C/A code phase vs. time is shown in Fig. 4. The data shows a globally negative slope. This slope is defined as the initial code phase velocity. The polarity of the slope can be explained as follows.

Let us assume that the true ADC sampling frequency is the nominal sampling frequency. If the Doppler frequency is also zero, i.e., there in no relative line-of-sight motion between the satellite and the receiver, the initial code phase vs. time would show a constant value over the time. That means that every millisecond of data block would show exactly the same initial code index. If the Doppler is positive, i.e., the satellite is approaching the receiver, the carrier received by the receiver is squeezed into a denser package compared to the case of zero Doppler. The initial code phase for one millisecond block of data would appear at a lesser value than that of the block precedes it in time. Therefore, the initial code phase vs. time would show a negative slope. Similarly, if the Doppler is negative, one would conclude that the initial code phase vs. time plot would show a positive slope using similar reasoning.

Now let us assume that the Doppler is zero. If the deviation of the sampling frequency from its nominal is positive, i.e., the true sampling rate is larger than the nominal value, the carrier wave will appear to spread out more in time than the case with zero deviation. One would conclude that the initial code phase vs. time slope is positive. Similarly, if the deviation in the sampling frequency is negative, one would conclude that the slope is negative.

Apparently, both the Doppler and the sampling frequency deviation affect the slope in the initial code phase vs. time plot. The typical result shown in Fig. 4 is for the case where the Doppler frequency is about -2000 Hz and the deviation of the sampling frequency is -2.6 Hz. In this case, the negative Doppler will result in positive initial code phase slope, while the negative sampling frequency deviation will lead to a negative initial code phase slope. As shown in the figure, the latter factor is the dominating factor and the final result is a negative slope.

To characterize the sampling frequency, one needs to resolve the effects due to two unknowns: sampling frequency deviation from nominal value and the signal Doppler frequency. We achieved the goal by solving a system of two equations with two unknowns. One equation is related to initial code phase velocity, and the other is related to carrier phase velocity, which will be discussed latter.

3. Formulation of the initial code phase velocity

Let the nominal sampling frequency be f_s and $a_0 = f_s T_0$, where T_0 is 1 millisecond (the period of C/A code). If this nominal value is the true sampling frequency, then, the measured Doppler will be the same as the true Doppler. In this case, the initial code phase $n(t)$ vs. time t is

$$n(t) = n_0 + \frac{-\gamma_d}{1+\gamma_d}\frac{a_0}{T_0}t \tag{1}$$

where n_0 is $n(0)$, and

$$\gamma_d = f_d / f_L \tag{2}$$

Here, f_d, f_L, and f_s are the Doppler, L1 carrier, and the receiver ADC sampling frequencies respectively. From (1), $n(t)$ vs. t shows a positive slope for a negative Doppler, and a negative slope for a positive Doppler, as is expected based on the qualitative discussions in the previous section.

If the nominal sampling frequency f_s is different from the true value f_s^{true} by δf_s, the slope of $n(t)$ vs. t can no longer be described by (1). The new formulation is the following:

$$n(t) = n_0 + \frac{\gamma_s - \gamma_d + \gamma_s\gamma_d}{(1-\gamma_s)(1+\gamma_d)} f_s t \tag{3}$$

where

$$\gamma_s = \delta f_s / f_s; \text{ and } \delta f_s = f_s^{true} - f_s \tag{4}$$

Therefore, the measured initial code phase velocity s can be obtained from (3) :

$$s = \frac{dn(t)}{dt} = \frac{\gamma_s - \gamma_d + \gamma_s\gamma_d}{(1-\gamma_s)(1+\gamma_d)} f_s \tag{5}$$

Equation (5) provides one of the two equations to solve for δf_s and f_d.

4. Formulation of the carrier phase velocity

The carrier phase vs. time provides the information to calculate the Doppler. Fig. 5 shows a typical carrier phase vs. time plot. The slope is the carrier phase velocity from which Doppler can be obtained. If the true system deviation in the sampling frequency is not zero, the measured Doppler will be different from the true Doppler. The relationship between the true and the measured Doppler is given by:

$$f_d = (f_d' + f_c')(1+\gamma_s) - f_c \tag{6}$$

where f_d' is the measured Doppler, f_c' is the nominal center frequency, and f_c is the true center frequency.

The relation between the f_c' and f_c can be deduced from the frequency plan of the circuit. A general form is given by:

$$f_c = f_c' - mf_s\gamma_s \tag{7}$$

where m is a parameter determined from the circuit's specific frequency plan. There are two receivers in this study. For the custom-designed receiver, the relation is given by:

$$f_c = 1.25MHz - 4f_s\gamma_s \tag{8}$$

For the commercially modified receiver, Equation (7) becomes:

$$f_c = 1.364MHz + 289f_s\gamma_s \tag{9}$$

Combining (6) and (7), we obtain the relation between the measured Doppler and the true Doppler:

$$f_d = (f_d' + f_c')(1+\gamma_s) - f_c' + mf_s\gamma_s \tag{10}$$

5. The solution for δf_s

Solving Equations (5) and (10), we obtain f_d and δf_s. The solution for δf_s is given by:

$$\begin{aligned}\delta f_S &= \gamma_S f_S \\ &= \frac{(mf_S + f_c' - f_L) f_S}{2(mf_S + f_c' + f_d')} \bullet \\ &\{1 - [1 - \frac{4(mf_S + f_c' + f_d')(f_d' + sf_L(s+f_S)^{-1})}{(mf_S + f_c' - f_L)^2}]^{0.5}\}\end{aligned} \tag{11}$$

Substituting f_c' and m from (8) and (9) for the commercial-modified and custom-designed receivers respectively into (11), δf_s can be calculated. Substitute the result into (10), we can obtain the true Doppler f_d.

IV. RESULTS AND DISCUSSIONS

Figs. 6 and 7 show typical results of the initial code phase vs. time for the custom-designed and the commercial-modified systems, respectively. The majority of data in Fig. 6 forms an apparent linear line. The scattered data points are due to a weak GPS signal which gives poor correlation results and can be removed using software routines. The slope of the line which is the apparent code phase velocity, can be obtained using a best fit routine. The majority of data points in Fig. 7 form three linear lines due to the repetitive nature of the initial code index. Comparing these two results, one notes that the commercial-modified system has a significantly larger initial code phase velocity than the custom designed one. This is because that the sampling rate deviation in the commercial-modified system is much larger than the one in the custom designed system. As will be seen latter, the commercial system has a sampling deviation in the order of 10^2 Hz, while the custom system one is only in the order of 10 Hz.

Fig. 8 and 9 show typical results of the carrier phase vs. time for the custom and commercial systems respectively. The slope at each point is the measured carrier angular velocity. From which one can calculate

the measured Doppler frequency. The curvature shown in the figure indicates a varying Doppler as time progresses.

The commercial system has only one frequency source and a series of multiplication and division circuits. It has a large $|m|$ (=*289*) value (see Eq. (9)). Because of this large m value, a small deviation of δf_s, e.g., in 10^2 Hz range, will result in a large deviation in f_c. Therefore, it is necessary to scan a wide range of possible Doppler frequencies during signal acquisition stage. The custom-designed system has two frequency sources to control the IF and sampling frequency separately. It has a small $|m|$ (= *4*) value (see Eq. (8)). A frequency deviation from the true f_s in the order of 10^2 Hz will not affect the deviation in f_c significantly. Furthermore, when mf_s and f_c' are much smaller compared to f_L, as is in the case of the custom-designed system, the solution in (11) can be simplified to:

$$\gamma_s = \frac{\delta f_s}{f_s} = \frac{s / f_s + f_d' / f_L}{1 - m f_s / f_L} \tag{12}$$

This approximation generates δf_s with value very close to the solution obtained from Eq. (11). For the custom-designed system, the difference in the δf_s values is within one tenth of 1Hz.

Fig. 10 shows the frequency deviation from the nominal sampling frequency vs. time for the custom-designed system. It shows a time series with a mean and a variance. The mean approaches the true sampling frequency deviation. This value can be obtained to an accuracy of less than 1 Hz with less than 0.5 second of data. The average frequency deviation approaches -12.6 Hz for our custom system based on our data analysis. This value is very close to the direct frequency measurement obtained using a frequency counter.

The conventional two-sample Allan variance analysis was performed on this time series. The result of the Allan variance vs. averaging time in log-log scale is shown in Fig. 11. The slope being close to two indicates that the noise process is of a phase modulation nature in the measured time frame from 10^{-3} to 10^{1} seconds.

Fig. 12 shows the frequency deviation from the nominal sampling frequency vs. time for the commercial-modified system. The average frequency deviation is about -353.6 Hz. The result of the Allan variance vs. averaging time in log-log scale is shown in Fig. 13. The figure shows a similar magnitude to the slope in Fig. 11. It seems that the frequency stability analysis using this method yields similar results to that of the Allan variance method regardless of the quality of the frequency sources. The reason may be due to possible dominant noise process occurring at the peripheral devices other than the oscillators. Those peripheral devices include the high gain amplifiers to amplify the weak GPS signals. The amplifiers are known to generate phase modulation in the stochastic process [2].

ACKNOWLEDGEMENT

We would like to thank the support of the Sensor Directorate of Air Force Research Laboratory.

REFERENCES

1. J. B. Tsui, "Fundamentals of Global Positioning System Receivers: A Software Approach", 2nd edition, John Willey and Sons, Inc., New York, 2004.

2. D. A. Howe, D. W. Allan and J. A. Barnes, "Properties of Signal Sources and Measurement Methods", NIST technical Note 1337, pp. TN-14, 1990.

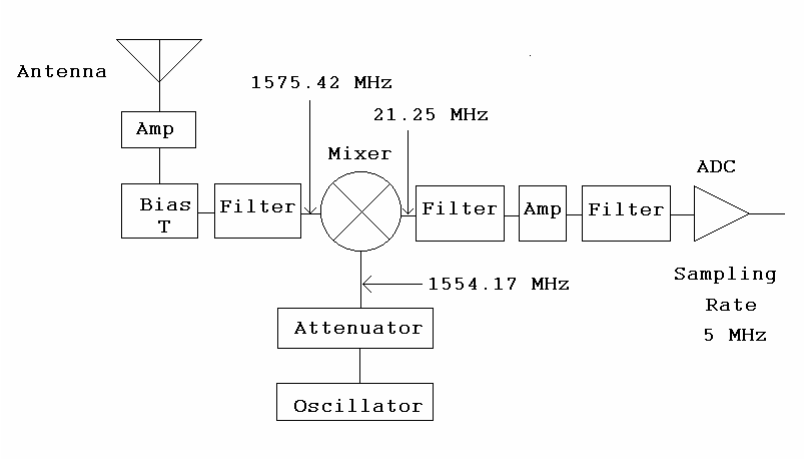

Fig. 1, a schematic of the custom designed GPS software receiver front-end.

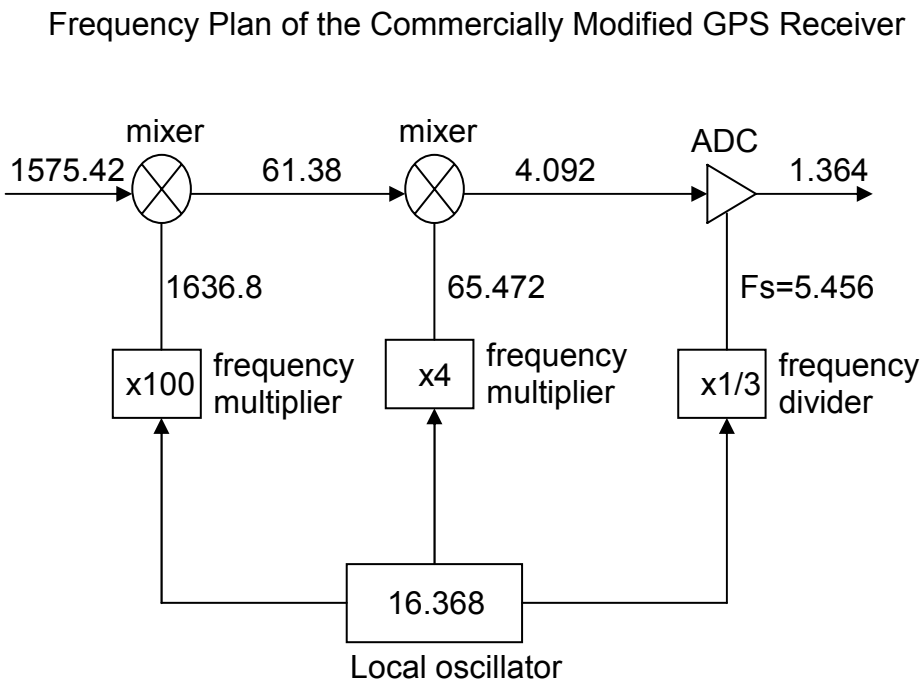

Fig. 2 the frequency plan of the commercial modified GPS software receiver. The frequency unit is MHz.

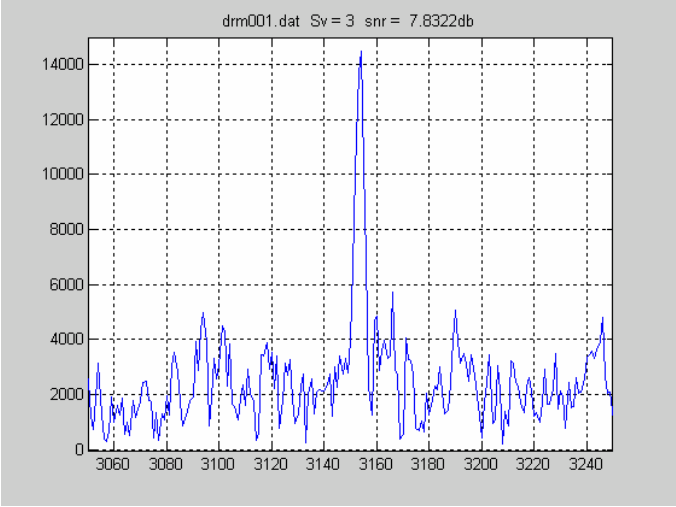

Fig.3, A typical correlation result to obtain initial code phase in one millisecond data block. The x-axis is the digitized data sequence in one-millisecond block, and the y-axis is the correlation strength.

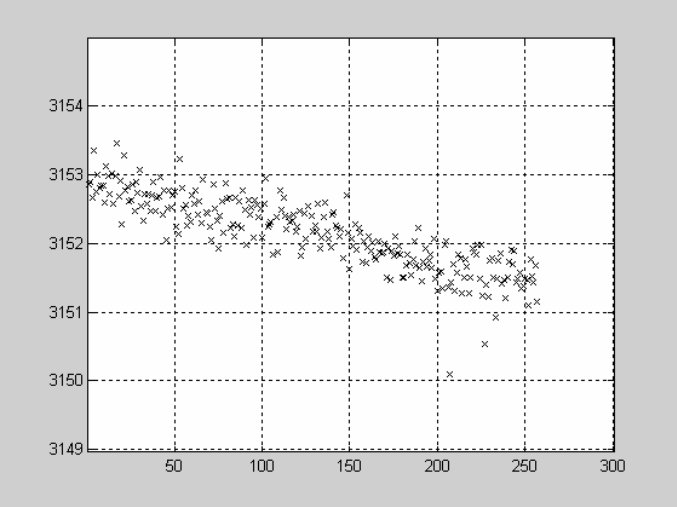

Fig. 4, A typical results of the initial-code-phase vs. time (in millisecond).

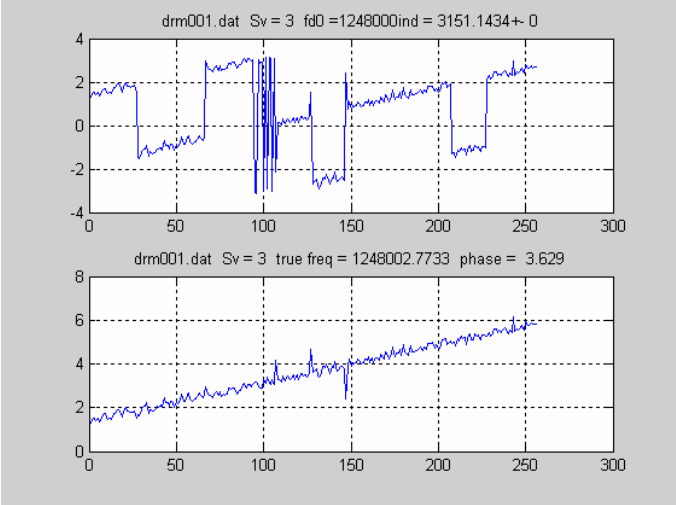

Fig. 5, the carrier phase vs. time (in millisecond) with (above figure) and without (bottom figure) the bi-phase due to navigation bits.

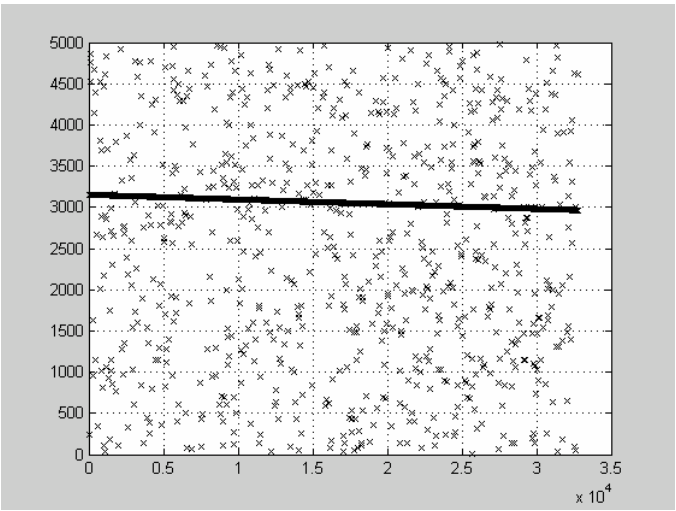

Figure 6, the initial C/A code phase vs. time in millisecond for the custom-designed system.

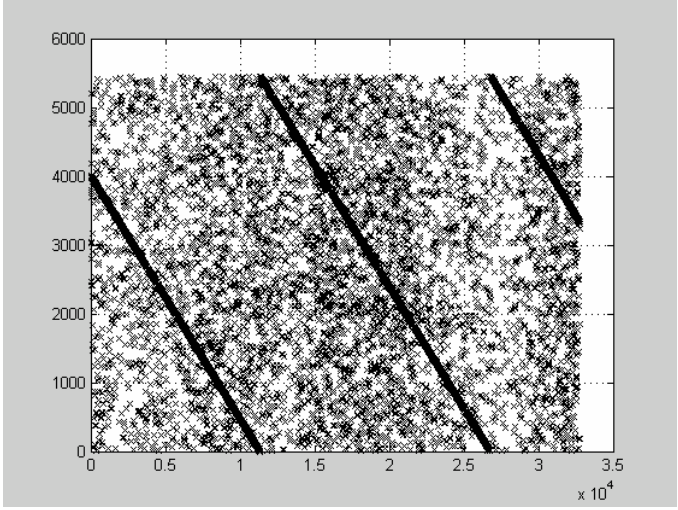

Fig. 7 the initial C/A code phase vs. time in millisecond for the commercial-modified system.

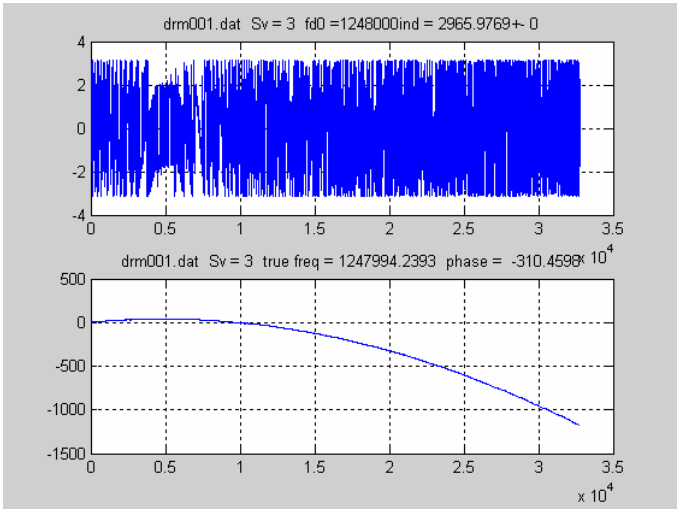

Fig. 8, the navigation code (upper figure) and the carrier phase (lower figure) vs. time in millisecond for the custom-designed system.

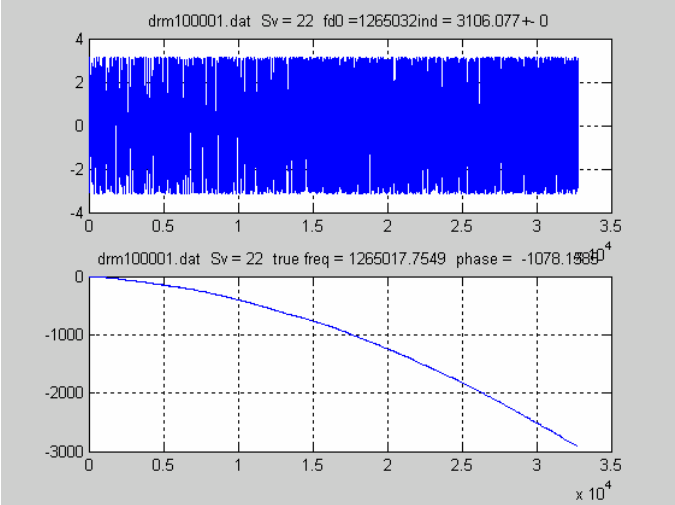

Fig. 9, the navigation code (upper figure) and the carrier phase (lower figure) vs. time in milli-second for the commercial-modified system.

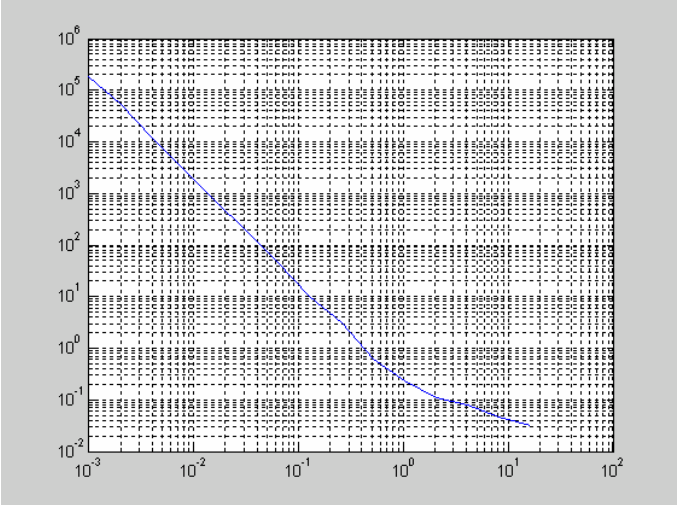

Fig. 11, The two-sample Allan Variance of the deviation frequency vs. averaging time in second for the custom-designed system.

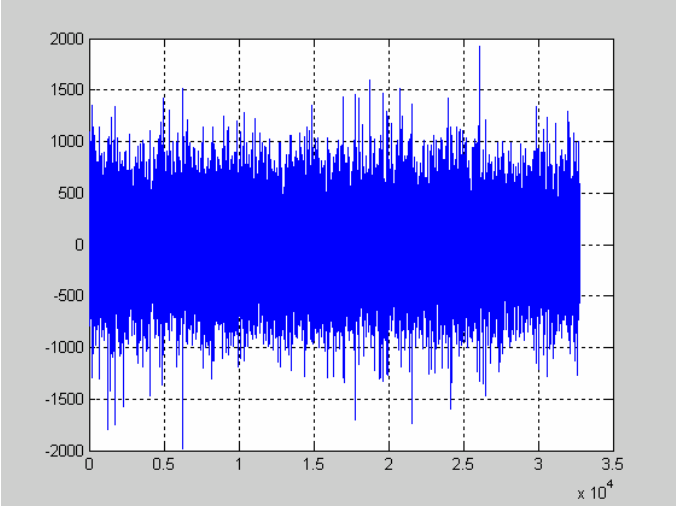

Fig. 10, the frequency deviation from the nominal operation frequency (5 MHz) vs. time in millisecond for the custom-designed system.

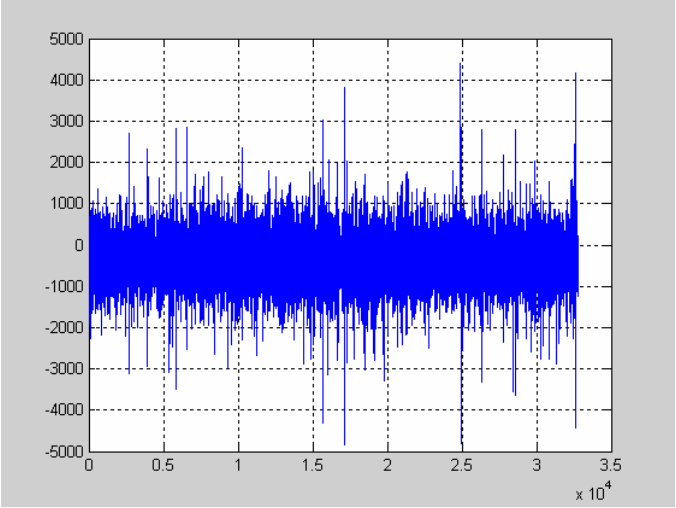

Fig. 12, the frequency deviation from the nominal operation frequency (5.456 MHz) vs. time in millisecond for the commercial-modified system. The mean deviation is -353.6 Hz.

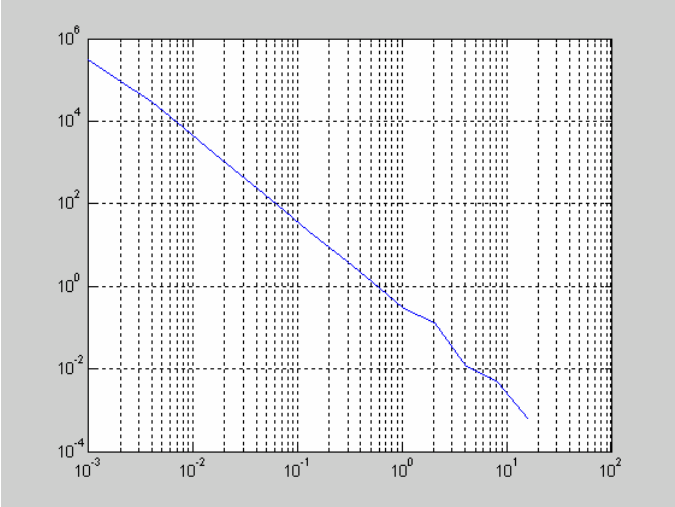

Fig. 13 The two-sample Allan Variance of the deviation frequency vs. averaging time in second for the commercial-modified system.